



Visualization and identification of single meteoritic organic molecules by atomic force microscopy

Katharina KAISER ¹, Fabian SCHULZ ^{1,11}, Julien F. MAILLARD², Felix HERMANN¹, Iago POZO ³, Diego PEÑA ³, H. James CLEAVES II ^{4,5}, Aaron S. BURTON ⁶, Gregoire DANGER^{7,8,9}, Carlos AFONSO², Scott SANDFORD ¹⁰, and Leo GROSS ^{*1}

¹IBM Research—Zurich, Rüschlikon 8003, Switzerland

²Normandie Univ, COBRA, UMR 6014 et FR 3038 Univ Rouen, INSA Rouen, CNRS IRCOF, 1 Rue Tesnière, Mont-Saint-Aignan Cedex 76821, France

³Departamento de Química Orgánica, Centro Singular de Investigación en Química Biolóxica e Materiais Moleculares (CiQUS), Universidade de Santiago de Compostela, Santiago de Compostela 15782, Spain

⁴Earth-Life Science Institute, Tokyo Institute of Technology, 2-12-1-IE-1 Ookayama, Meguro-ku, Tokyo 152-8550, Japan

⁵Blue Marble Space Institute for Science, 1001 4th Ave, Suite 3201, Seattle, Washington 98154, USA

⁶Astromaterials Research and Exploration Science Division, NASA Johnson Space Center, MS XI-3, Houston, Texas 77058, USA

⁷Laboratoire de Physique des Interactions Ioniques et Moléculaires (PIIM), CNRS, Aix-Marseille Université, Marseille, France

⁸CNRS, CNES, LAM, Aix-Marseille Université, Marseille, France

⁹Institut Universitaire de France, Paris, France

¹⁰Space Science Division, NASA Ames Research Center, MS 245-6, Moffett Field, California 94035, USA

¹¹Present Address: Fritz Haber Institute of the Max Planck Society, Berlin 14195, Germany

*Corresponding author. E-mail: lgr@zurich.ibm.com

(Received 22 September 2021; revision accepted 16 December 2021)

Abstract—Using high-resolution atomic force microscopy (AFM) with CO-functionalized tips, we atomically resolved individual molecules from Murchison meteorite samples. We analyzed powdered Murchison meteorite material directly, as well as processed extracts that we prepared to facilitate characterization by AFM. From the untreated Murchison sample, we resolved very few molecules, as the sample contained mostly small molecules that could not be identified by AFM. By contrast, using a procedure based on several trituration and extraction steps with organic solvents, we isolated a fraction enriched in larger organic compounds. The treatment increased the fraction of molecules that could be resolved by AFM, allowing us to identify organic constituents and molecular moieties, such as polycyclic aromatic hydrocarbons and aliphatic chains. The AFM measurements are complemented by high-resolution mass spectrometry analysis of Murchison fractions. We provide a proof of principle that AFM can be used to image and identify individual organic molecules from meteorites and propose a method for extracting and preparing meteorite samples for their investigation by AFM. We discuss the challenges and prospects of this approach to study extraterrestrial samples based on single-molecule identification.

INTRODUCTION

Meteorites are key samples from which one can obtain clues on the origin of the solar system. Carbonaceous chondrites are among the most primitive solar system materials available, with many having experienced minimal alteration since their formation (Brearley, 2006). While the mineral phases of these

meteorites provide information on the alteration history of their parent bodies, their organic matter, representing up to 5% of their weight (Glavin et al., 2018; Pearson et al., 2006; Pizzarello et al., 2006), gives invaluable information on the organic content that could have been delivered to the early Earth. This organic matter can be divided into two fractions: soluble organic matter (SOM), which represents up to 25% of the

organic content, and the dominant insoluble organic matter (IOM) fraction, which contains the balance of organic carbon (Alexander et al., 2007; Cody & Alexander, 2005; Sephton, 2002).

The SOM is generally recovered by washing meteorite powders with ultrapure water, aqueous acidic or basic solutions, or organic solvents, typically at elevated temperatures. The extracts are then characterized with various analytical methods. For example, targeted analyses with chromatography techniques coupled to mass spectrometry have identified a wide variety of organic molecules (Pizzarello et al., 2006), including amino acids (e.g., Elsila et al., 2016), carboxylic and dicarboxylic acids (aromatic and aliphatic; Huang et al., 2005; Pizzarello & Huang, 2002; Pizzarello et al., 2001), nucleobases (Callahan et al., 2011), sugars (Cooper et al., 2001; Furukawa et al., 2019), aliphatic and aromatic hydrocarbons (e.g., Elsila et al., 2005; Sephton, 2002; Sephton et al., 2001), aliphatic amines (Aponte et al., 2014), aliphatic hydroxycarboxylic acids (Aponte et al., 2020), aldehydes and ketones (Aponte et al., 2019; Simkus et al., 2019), and a host of other classes of compounds (see Glavin et al. 2018) and references therein for a recent review). A range of polycyclic aromatic hydrocarbons (PAHs) have also been identified, showing the vast chemical diversity present in such objects (Sephton, 2002). This molecular diversity has been further revealed by the analysis of SOM extracts with a high-resolution mass spectrometry apparatus in 2010 (Schmitt-Kopplin et al., 2010). One of the most studied meteorites is the carbonaceous chondrite Murchison that fell in Australia in 1969 near Murchison, Victoria. After extraction of Murchison meteorite powders with several organic solvents, analysis by direct infusion Fourier transform ion cyclotron resonance mass spectrometry (FTICR-MS) via electrospray ionization revealed unique mass species representing more than 14,000 molecular formulas. Assuming typical known isomerism among organic species, it was suggested that these compounds with unique formulas could represent an order of magnitude greater number of individual unique isomers (Schmitt-Kopplin et al., 2010), a finding supported by the work of Ruf et al. (2019). The molecular diversity observed in meteoritic SOM is only rivalled on Earth by degraded organic material such as natural dissolved organic matter and crude petroleum (Schmitt-Kopplin et al., 2019). Because of their molecular diversity and the presence of molecules of biological interest (e.g., amino acids, sugars, and nucleobases), meteorite organics have been considered a potentially important reservoir of prebiotic organic material on early Earth (Chyba et al., 1990; Oró, 1961; Pizzarello, 2007; Sandford et al., 2020).

The isolation of the IOM fraction from meteorites requires a chemical treatment stronger than that for the soluble fraction, including a demineralization step. Due to the IOM fraction's insolubility, different analytical techniques are used for its study (Alexander et al., 1998, 2017; Cody & Alexander, 2005). IOM is suggested to consist of aggregates of macromolecules composed of small condensed aromatic units linked by aliphatic bridges, including a small fraction of heteroatoms (Cody & Alexander, 2005; Derenne & Robert, 2010; Remusat et al., 2005) and fractions of small polyaromatic moieties with masses ranging from 200 to 1000 Da (Danger et al., 2020).

Atomic force microscopy (AFM) could complement analyses of meteorite organic matter, and other samples of extraterrestrial origin, by resolving the actual structures of single organic molecules within the overall molecular population.

Recently, high-resolution noncontact AFM with CO-functionalized tips (Gross et al., 2009) was used to study complex molecular mixtures on the basis of atomically resolving single molecules (Commodo et al., 2019; de Oteyza et al., 2013; Fatayer et al., 2018; Schuler, Fatayer, et al., 2017; Schuler, Meyer, et al., 2015; Schulz et al., 2021), and this technique has been employed to identify a priori unknown molecules (Gross et al., 2010; Hanssen et al., 2012; Schuler, Meyer, et al., 2015). Obtaining atomic resolution and identifying individual compounds by AFM effectively complements the information obtained using nuclear magnetic resonance (NMR), gas chromatography, and FTICR-MS on complex heterogeneous mixtures of molecules (Schuler, Fatayer, et al., 2017).

Although a direct quantification is almost impossible with AFM, it can complement the established techniques. Noncontact AFM can detect and resolve very rare species in samples, facilitated by its single-molecule sensitivity. Furthermore, AFM can assist isomer-specific structure identification of proton-poor compounds, which are challenging to resolve by MS and NMR (see Gross et al., 2010; Hanssen et al., 2012).

In the context of astrophysics, laboratory analogs of interstellar organic material (Martínez et al., 2020; Santoro et al., 2020) and analogs of Titan's haze (Schulz et al., 2021) have been studied previously by AFM. However, samples of extraterrestrial origin have not been atomically resolved by noncontact AFM to date. Here, we attempted to study molecules from the Murchison meteorite using noncontact AFM to explore the prospects of this method to investigate samples from meteorites or other samples of extraterrestrial origin, for example, samples recovered by extraterrestrial sample return missions.

EXPERIMENT

One challenge of studying organic compounds from meteorites is the limited availability of sample material. The amount of meteorite material is finite; the organic components comprise only a small fraction of the sample mass, and the SOM is only a fraction of the organic material. Although noncontact AFM resolves single molecules, organic material in the order of 0.1 mg is required (and consumed) to prepare a sample for its AFM investigation in our experimental setup (Schuler, Mohn, et al., 2015).

To obtain atomic resolution of the molecules, we use noncontact AFM in the frequency-modulation mode (Albrecht et al., 1991), abbreviated as AFM hereafter. We image the molecules in constant height mode, scanning the tip along a plane parallel to the surface, above the molecule with a CO-functionalized tip (Gross et al., 2009). The CO functionalization provides atomic resolution because of its inertness, allowing us to probe repulsive forces above the molecules. In addition, relaxations of the CO at the tip enhance the contrast (Gross et al., 2012; Hapala et al., 2014). The AFM images show a map of the frequency shift of the oscillating cantilever. The molecular structure reveals itself as a bright modulation due to repulsive forces, on top of a dark background due to attractive forces (Gross et al., 2009). The repulsive contrast above atoms and bonds, which reveals the molecular structure, is a consequence of Pauli repulsion between the CO molecule at the tip and regions of increased electron density of the imaged molecule (Moll et al., 2010). Molecular structures and moieties can often be assigned by comparison with AFM measurements of known model compounds. For most structures, several images at different tip heights were obtained to facilitate the structural assignment with high confidence (see supporting information).

AFM is best suited to image and identify the structure of relatively planar molecules (Gross et al., 2018; Schuler, Meyer, et al., 2015; Schuler et al., 2020). As a result of the preparation method, in which the molecules are sublimed onto the sample in ultra-high vacuum (UHV) by resistive flash heating from a piece of oxidized silicon wafer (Schuler, Meyer, et al., 2015; Schuler et al., 2020), large and fragile molecules tend to fragment before they sublime. The flash heating technique enhances volatility by favoring sublimation and suppressing competitive fragmentation (Beuhler et al., 1974; Rapenne et al., 2006). Fragmentation typically becomes an issue for molecular weights exceeding 700 Da (Schuler, Meyer, et al., 2015; Schuler et al., 2020). Control experiments

for several aliphatic compounds, featuring aliphatic PAH groups and aliphatic chains, showed that they are not dehydrogenated by the flash heating deposition (Schuler, Zhang, et al., 2017).

The limitation to planar systems stems from the extreme surface sensitivity of the AFM imaging technique. The atomic contrast obtained by AFM is related to Pauli repulsion (Moll et al., 2010) and therefore is extremely short ranged, resolving only the topmost layer of atoms of a surface or a molecule. Because of this, nonplanar molecules are challenging to identify and require special data acquisition modes (Albrecht et al., 2015; Gross et al., 2010; Martin-Jimenez et al., 2019; Mohn et al., 2011; Moreno et al., 2015). In addition, some molecules, mainly small ones, have a low diffusion barrier on the surface, and they are often displaced by the AFM tip when attempting to resolve them with atomic resolution.

AFM provides some elemental sensitivity in planar molecules, established by investigating known model compounds (Gross et al., 2010; Moll et al., 2012; Schuler et al., 2013; Schulz et al., 2018, 2021; Van Der Heijden et al., 2016; Zahl & Zhang, 2019). Typically, N heteroatoms result in slightly fainter (less repulsive) contrast compared to C atoms (Schulz et al., 2018, 2021; Van Der Heijden et al., 2016; Zahl & Zhang, 2019), whereas O atoms show an attractive contrast that can be explained by the electron density decaying more rapidly with distance (dark in AFM images that show atomic contrast of the PAH molecular core) compared to C and N atoms (Gross et al., 2010; Moll et al., 2012; Pavliček et al., 2017; Schuler et al., 2013). S atoms, due to their larger Van der Waals radius exhibit greater repulsion, setting in at a larger tip height compared to N, C, and O (Zahl & Zhang, 2019). In addition, several nonplanar moieties, such as CH₂ groups (Schuler et al., 2013; Schuler, Zhang, et al., 2017), methyl groups (Commodo et al., 2019; Schuler, Meyer, et al., 2015), aliphatic chains (Schuler, Zhang, et al., 2017), and methoxy moieties (Hanssen et al., 2012) can be assigned by comparison with previously measured compounds.

For complex molecular mixtures studied previously in the field of petroleum chemistry, the comparison of AFM-identified molecular structures with high-resolution mass spectrometry data confirmed the representativeness of the AFM measurements (Schuler, Fatayer, et al., 2017; Zhang et al., 2018).

RESULTS

We first prepared a sample by putting ground, unprocessed material (UM) of Murchison on a Si wafer and subliming it onto a Cu(111) surface that was

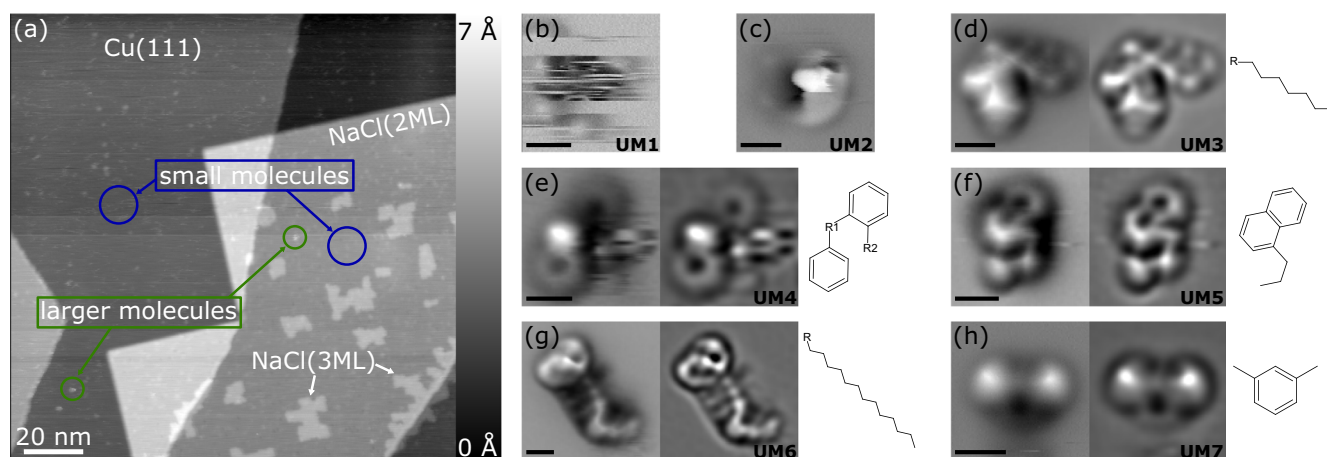


Fig. 1. Unprocessed Murchison (UM) meteorite sample investigated by AFM, prepared on Cu(111) partly covered by NaCl islands. a) Constant current STM overview; sample voltage $V = 0.5$ V, tunneling current $I = 1$ pA. b–h) Constant height high-resolution AFM measurements with a CO tip of individual molecules of the unprocessed Murchison sample (UM1–UM7). For molecules UM3–UM7 (e–h), the raw data (respective left panels), corresponding Laplace filtered, i.e., high-pass filtered, image (respective center panels) and proposed structure (respective right panels) are shown, where R denotes unassigned moieties. (b) and (c) are exemplary images of small molecules. (d) to (h) are images of larger molecules. The scale bars in (b) to (h) correspond to 0.5 nm. (Color figure can be viewed at wileyonlinelibrary.com.)

partially covered by (100)-oriented NaCl islands of two and three monolayer (ML) thickness. The NaCl islands were prepared to facilitate CO functionalization of the tip. Figure 1a shows an overview of the surface prepared in this manner obtained by scanning tunneling microscopy (STM). Most of the adsorbates imaged by AFM and STM exhibit lateral dimensions of ≤ 1 nm, which we define in the context of this study as “small molecules.” These small molecules could not be identified by AFM. Often, when trying to obtain atomic resolution of such small molecules, they get displaced by the tip during imaging (see, e.g., Fig. 1b). If stable imaging was possible, the small molecules were typically resolved as features that could not be assigned (see, e.g., Fig. 1c).

Some comparably larger molecules are also observed in the UM fraction (Fig. 1a, labelled “larger molecules”). We could obtain atomic resolution on some of the larger molecules by AFM, as shown in Figs. 1d–h. The proposed structures for such molecules are shown in Fig. 1. We resolved molecules featuring two (UM4 and UM5, Figs. 1e and 1f) and one (UM7, Fig. 1h) carbon rings. In addition, we observed molecules that contained aliphatic $-(CH)_2-$ chains (UM3 and UM6, Figs. 1d and 1g) and methyl groups (UM7, Fig. 1h) assigned by comparison with previously resolved model compounds (Commodo et al., 2019; Schuler, Meyer, et al., 2015; Schuler, Zhang, et al., 2017). In Fig. 1d, the left part of the molecule could not be assigned unambiguously because

of its nonplanarity. This part probably corresponds to an aliphatic chain in a twisted conformation (Schuler, Zhang, et al., 2017). Small NaCl islands are distinguished from molecules by high-resolution AFM images (Schuler et al., 2016).

Some of the larger molecules were also too mobile to be resolved. As a trend, however, with exceptions, the adsorption energy increases and the on-surface mobility decreases with increasing size of molecules. The on-surface diffusion barrier and thus the mobility of molecules depend on the exact structure of the molecule and the surface. During our measurements, small molecules were often picked up by the tip, which required the preparation of a clean and stable tip before measurements could be continued. The frequent tip degradations caused by the small molecules made the investigation of this sample tedious, time consuming, and challenging.

We attempted to extract a fraction of the meteorite sample that contained an increased ratio of molecules that can be resolved by AFM, and fewer of the small molecules that cause tip degradation. To that end, we treated a fraction of the UM with a sequence of trituration and extraction procedures using organic solvents. First, we performed consecutive trituration steps of the solid sample employing methanol, hexane, and dichloromethane to remove most of the small molecules detected in the UM sample. In each step, the sample was sonicated for 2 min before centrifugation of the suspension and decantation of the solvent. The

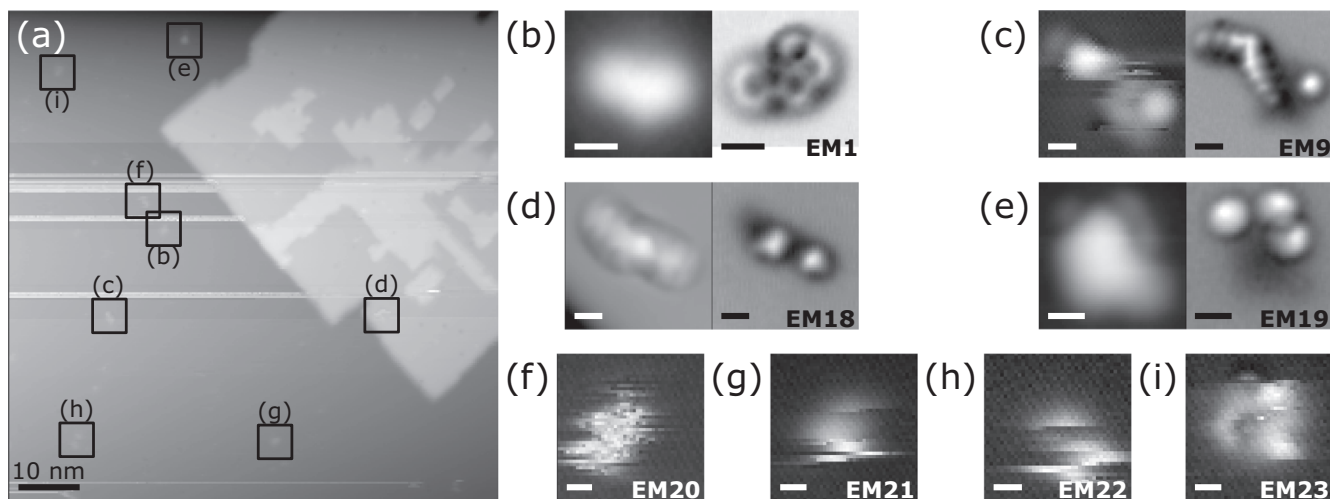


Fig. 2. Extracted Murchison (EM) meteorite sample, prepared on Ag(111) partly covered by NaCl islands. a) Constant current STM overview; $V = 0.4$ V, $I = 1$ pA. b–i) High-resolution measurements with a CO tip on all the individual molecules labelled in (a). For molecules (b) to (e), both STM (left panels) and AFM (right panels) data are shown (EM1, EM9, EM18, EM19). Molecules labelled (f) to (i) were too mobile to be resolved and only STM measurements are shown (EM20–EM23).

resulting solid was then extracted in chlorobenzene in a Soxhlet apparatus for 20 h. Finally, the chlorobenzene solution and the residual solid (RM) were separated, and the solution was concentrated under reduced pressure to obtain the extracted Murchison (EM) meteorite sample.

For AFM analysis, about 0.5 mg of the extracted EM fraction was sublimed in front of a Ag(111) single crystal partially covered by bilayer (100)-oriented NaCl islands. Note that here we used a single Ag crystal, but we do not expect that changing the sample from Cu (111) to Ag(111) affected the results concerning the structures of the observed molecules.

An STM overview image of the sample prepared with the EM fraction is shown in Fig. 2a. We observed that, compared to the sample prepared from the unprocessed material, the fraction of larger molecules increased and that of smaller molecules decreased significantly. For UM, we observed a ratio of large to small molecules in the order of 10^{-3} to 10^{-2} , while for EM, this ratio was in the order of 10^{-1} to 1. To obtain these ratios, we roughly estimated the number of small molecules (with lateral dimensions of ≤ 1 nm) and counted the number of larger molecules (> 1 nm) in STM overview images, such as the ones shown in Figs. 1a and 2a.

Figures 2b–i show high-resolution images of all the larger molecules marked in Fig. 2a, providing an unbiased random sample of the molecules prepared on the surface. Among these molecules, we resolved a PAH with four rings (EM1, Fig. 2b) and an aliphatic chain (EM9, Fig. 2c). Molecule EM18 (Fig. 2d) probably also features an aliphatic chain, as indicated by the STM

measurement; however, we could not approach the molecule with the tip close enough to resolve it. Molecule EM19 could not be resolved because it was too nonplanar (see Fig. 2e). Four of the eight molecules were too mobile and were displaced when attempting atomically resolved imaging (EM20–EM23, Figs. 2f–g), similar to the small molecules that were predominant in the UM sample.

Figure 3 shows molecules from the EM fraction that could partly be resolved by AFM, together with proposed structures. We assigned PAHs with four rings exhibiting a backbone of 2,3-benzocarbazole (EM1, Fig. 3a), pyrene (EM2 and EM4, Figs. 3b and 3d), and benz[a]anthracene (EM3, Fig. 3c). The nitrogen heteroatom in EM1 (Fig. 3a) is tentatively assigned because of its slightly smaller Δf contrast compared to C atoms (Schulz et al., 2018, 2021; Van Der Heijden et al., 2016; Zahl & Zhang, 2019). We assign the bright features in Fig. 3c in the lower right side of the image and in Fig. 3e on the upper part of the image, to small adsorbates that are not covalently bonded to the EM3 and EM5, because of their apparent distance to EM3 and EM5, respectively. The dark contrast of the bottom right ring of EM4 might indicate that EM4 could be a substituted pyrene (compare with the unsubstituted pyrene EM2). We tentatively relate the contrast of that ring to an unknown side group attached to that ring. We identified trans-stilbene (EM5, Fig. 3e), which contains two phenyl groups linked with an ethylene bridge; see supporting information for AFM simulations. Several molecules contained one carbon ring, with either one or two side groups attached to it; see Fig. 3f (EM6),

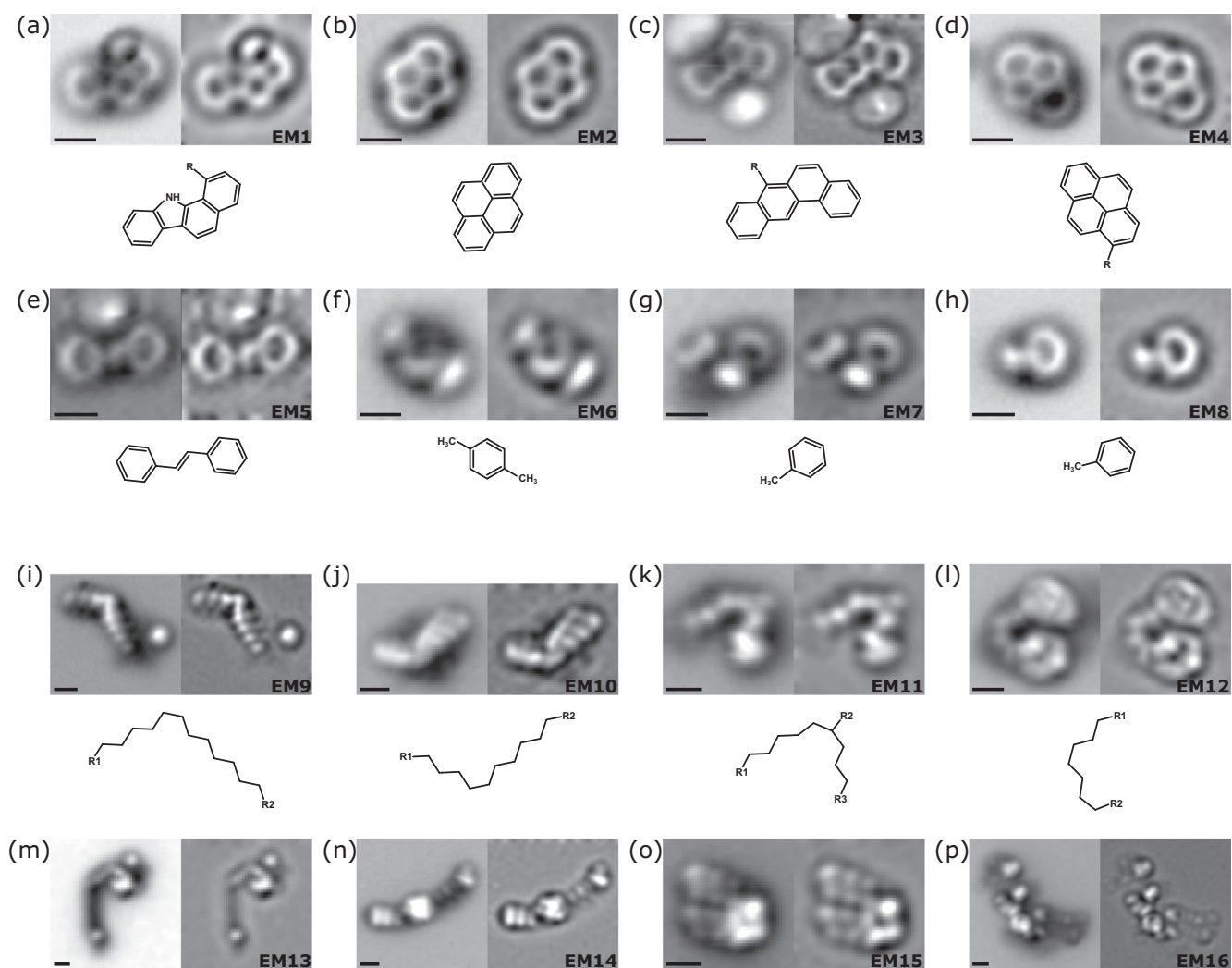


Fig. 3. Extracted Murchison sample, constant height AFM measurements with a CO tip of individual molecules. For EM1–EM12 (a–l) a proposed structure is shown, where R denotes unassigned moieties. EM13–EM16 (m–p) consist mainly of chains and structure assignment was not possible with reasonable confidence. For all molecules AFM raw data (respective left panels) and the corresponding Laplace filtered, i.e., high-pass filtered, images (respective right panels) are shown. All scale bars correspond to 0.5 nm.

and Figs. 3g and 3h (EM7, EM8), respectively. For the molecules in Figs. 3f–h and UM7 in Fig. 1h, we tentatively assigned those side groups to methyl groups by comparison with imaged model compounds (Commodo et al., 2019; Schuler et al., 2015; Zahl & Zhang, 2019). In addition, we found several molecules which we assign as aliphatic chains (Schuler, Zhang, et al., 2017), shown in Figs. 3i–o (EM9–EM15). Often, these chains featured nonplanar moieties that we could not assign (EM11–EM16, Figs. 3k–p). The end groups of the aliphatic chains in Figs. 3i–k denoted as R₁, R₂, and R₃ are likely CH₃ groups and the end groups in Fig. 3l are likely aliphatic hexagonal carbon rings. For these molecules, measurements of known model compounds, i.e., aliphatic chains with such end groups,

could corroborate the structural assignment in the future. Some molecules were too nonplanar to be resolved, for example, EM16, and those were often of comparably large size.

To complement our AFM analysis, we conducted LDI-FTICR-MS (laser desorption ion cyclotron resonance mass spectrometry) on EM and on the RM. The obtained spectra are shown in Fig. 4. In both analyses, a multitude of signals was detected, highlighting the complexity of each fraction. It can be observed that the distribution of EM is shifted to higher masses compared to the RM spectrum. A zoom-in between m/z 265.0 and m/z 265.3 (insets in Fig. 4) reveals significant differences in the chemical compositions of the two samples.

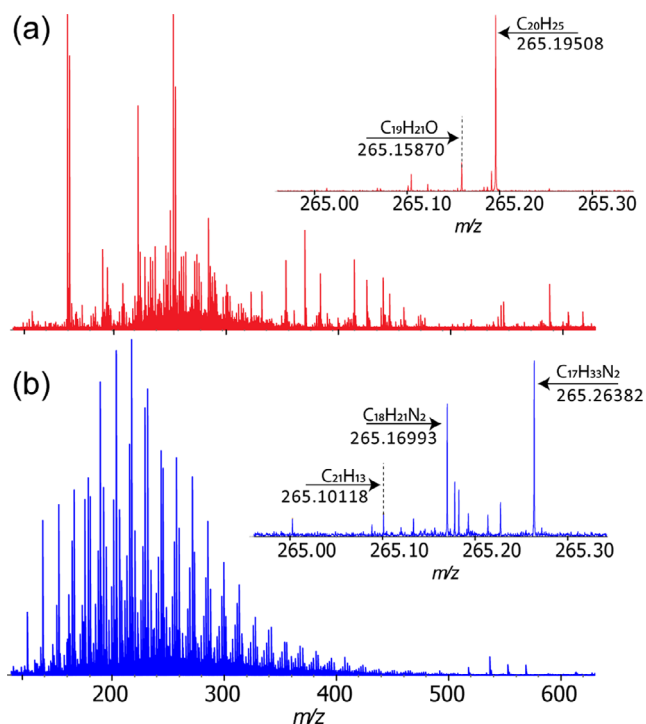


Fig. 4. LDI-FTICR-MS of (a) chlorobenzene extracted residue of Murchison, EM and (b) solid residual after extraction, RM. (Color figure can be viewed at wileyonlinelibrary.com.)

To further elucidate the fraction differences, double bond equivalent (DBE) versus carbon number ($C\#$) diagrams were used. The DBE value is calculated as $DBE = c - h/2 + n/2 + 1$ for a $C_cH_hN_nO_oS_s$ molecular formula. These plots were used to compare complex mixtures such as petroleum (Stanford et al., 2006) and to facilitate a quick observation of differences between chemical families. Figure 5 shows the obtained DBE versus $C\#$ maps for the C_xH_y family (Figs. 5a and 5b) and for the $C_xH_yN_1$ family (Figs. 5c and 5d) for EM and RM. For each graphic, the PAH line was added. This family of compounds is generally added to facilitate the comparison between cartographies (Cho et al., 2011). For the C_xH_y hydrocarbon family, the fingerprints are very different between EM and RM. The residual solid RM presents a large content of highly aromatic species, whereas the extract EM shows comparably more aliphatic species. For the $C_xH_yN_1$ species, the fingerprint is narrower in EM with the most intense species located between DBE values of 11 and 13. Both the variety and the proportion of molecules containing N as heteroatoms is reduced in EM with respect to RM (see insets in Fig. 4). Oxygen- and sulfur-containing species were also detected and their DBE versus C maps are presented in the supporting information. We found that EM contained a larger diversity of O- and S-containing species compared to RM.

A larger mean molecular size and smaller proportions of species with masses below 200 Da are detected in EM compared to RM (see Fig. 4), which is consistent with the better characterizability of EM compared to UM by AFM (cf. Figs. 1a and 2a). To each DBE map, one putative structure is given for each most intense region of detected species. The most intense regions found by mass spectrometry include molecular structures that are similar to those that could be resolved with AFM in EM and UM.

DISCUSSION

The MS results support that the structures we observed by AFM are representative. Moreover, the MS results confirm the decrease of small organic molecules in EM with respect to UM that we aimed for in order to obtain a fraction that could be better investigated by AFM. Note that LDI does not allow the ionization of alkanes, which are observed in AFM. Comparing our results with the literature on the Murchison meteorite supports that molecular structures of Murchison were imaged by AFM. Various PAHs have been identified by several analytical methods in various meteorites and particularly in Murchison. The most abundant PAHs observed in Murchison were pyrene, fluoranthene, phenanthrene, and acenaphthene (Basile et al., 1984; Pering & Ponnampereuma, 1971). This supports that the pyrene (EM2, Fig. 3b) observed with our AFM analyses can be related to the meteorite organics. Furthermore, benzanthracene derivatives were also identified, as would be expected for a suite of PAHs of extraterrestrial origin, supporting the meteoritic origin of the EM3 compound (Fig. 3c) (Basile et al., 1984). Low molecular weight aromatic compounds such as benzene, toluene, or xylene derivatives have also been identified in Murchison (Sephton et al., 1998). In addition, methylated derivatives of small PAH compounds such as naphthalene have been detected in several meteorites, including Murchison (Elsila et al., 2005) supporting the possible meteoritic origin of compounds EM6, EM7, and EM8 (Figs. 3f–h). Our MS results indicate oxygen and sulfur heteroatoms within the samples. In the molecules that we resolved by AFM, we did not observe those heteroatoms, which would typically be indicated by their characteristic AFM contrast (Gross et al., 2010; Moll et al., 2012; Pavliček et al., 2017; Schuler et al., 2013; Zahl & Zhang, 2019). Presumably, we did not observe these heteroatoms, because of the small number of molecules that we resolved by AFM. Finally, various alkane chains were also identified by the AFM analyses. Hydrocarbons are frequently observed in various meteorites and particularly in Murchison. However, their endogenous

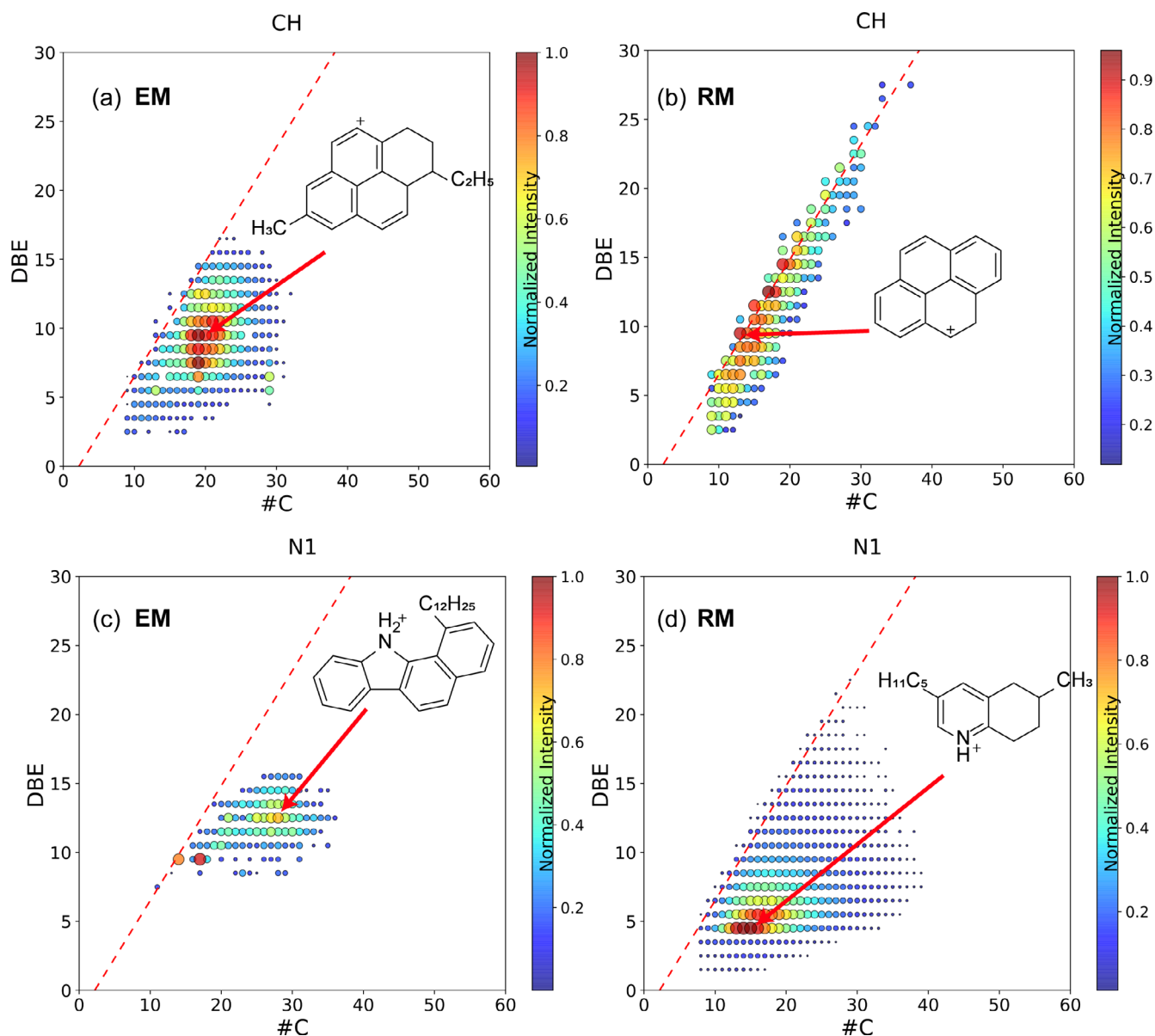


Fig. 5. Double bond equivalent (DBE) versus carbon number representation of the extracted solution EM (left) and the residual solid after extraction RM (right). (a) and (b) C_xH_y family, (c) and (d) $C_xH_yN_1$ family. Straight lines represent the polycyclic aromatic hydrocarbons family. One putative structure is given for each most intense region. (Color figure can be viewed at wileyonlinelibrary.com.)

origin is still debated since their even-odd carbon distribution and/or their carbon isotopic composition ($\delta^{13}C$ values) cannot rule out a potential terrestrial contamination (Sephton, 2002).

Comparison of the AFM results with both MS data and with literature reports supports that structures we resolved were representative for organic molecules and/or moieties present indigenously in the Murchison meteorite. The single-molecule sensitivity of AFM provides a unique advantage when characterizing molecular mixtures and allows for resolving even rare

individual species. On the other hand, it is challenging to completely rule out the possibility that the molecules imaged are contaminants, as even a single-molecular contaminant could be resolved. Therefore, to increase the statistical significance, it is important to resolve many molecules and a large proportion of the molecules within a sample (e.g., Commodo et al., 2019; Schuler, Fatayer, et al., 2017). The extraction procedure that we used here (to obtain the EM fraction) helped us to resolve a larger proportion (compared to the untreated sample UM) of the molecules found on the surface after

preparation. The good agreement of the observed structures with those described in the literature and with the most intense peaks in our measured MS data provides support that the imaged molecules are from the meteorite and not contaminants. However, since even in the EM sample the number of resolved molecules was small, we cannot fully rule out that some of the molecules were contaminants.

In the future one aim to improve AFM for elucidation of meteorite molecules is to further improve the extraction process to obtain fractions that are even better suited for their AFM investigation, that is, fractions with a larger content of planar aromatic molecules that can be identified by AFM. This is especially challenging when the amount of material is limited as it is for meteorite samples or material from return missions. We hope that the results presented here, which showcase that it is possible to resolve individual molecules in extracts from meteorites, motivate further efforts to extract such fractions. Moreover, we aim to improve AFM identification to increase the number of species that can be resolved by AFM in general, that is, improved elemental sensitivity (Alldritt et al., 2020; Hanssen et al., 2012; Schulz et al., 2018; Van Der Heijden et al., 2016; Zahl & Zhang, 2019), improved imaging of three-dimensional, nonplanar molecules (Albrecht et al., 2015; Martin-Jimenez et al., 2019; Mohn et al., 2011; Moreno et al., 2015), and improved preparation methods (e.g., Hamann et al., 2011; Pawlak et al., 2019; Rauschenbach et al., 2009).

CONCLUSION

In conclusion, this work shows that single molecules from meteorite samples can be resolved by AFM after suitable sample preparation. The molecule classes we resolved by AFM have also been detected in meteorites in previous literature reports. The single-molecule sensitivity of AFM could in the future contribute to resolving new molecules and molecular architectures in meteorites and samples from return missions and could be a valuable complement to established techniques such as FTICR-MS and NMR. To that end, it would be desirable to further improve the extraction of samples for their AFM investigation and further improve molecular identification by AFM.

METHODS

Sample Extraction

A fraction from Murchison raw material was ground to powder (400 mg) and placed in a Teflon

tube, and 3 mL of methanol was added to it. The suspension was sonicated for 2 min and subsequently centrifuged and decanted, to obtain the solid and solution separately. This protocol was repeated twice with methanol (three times in total). Following the same experimental procedure, the resulting solid was subsequently triturated with hexane (3×3 mL) and dichloromethane (9×3 mL). The remaining solid was extracted with chlorobenzene (15 mL) using a Soxhlet apparatus for 20 h. Finally, the chlorobenzene solution and the residual solid (RM) were separated, and the solution was concentrated under reduced pressure to obtain the EM meteorite sample. The solvents used for the trituration steps (hexane, dichloromethane, and methanol) were purchased from Fisher (HPLC grade). The solvent used for the Soxhlet extraction (chlorobenzene) was purchased from ABCR (>99%) and purified by distillation before use. Note that chlorobenzene, which is used in the extraction of EM, and dichlorobenzene could yield a similar AFM contrast as methylbenzene and dimethylbenzene, respectively. Because we observed no traces of chlorobenzene and dichlorobenzene with FTICRMS in EM, we tentatively assigned the side groups of EM6, EM7, and EM8 (Figs. 3g and 3h) as methyl groups. In addition, we observed UM7 (Fig. 1h) featuring similar side groups in the untreated fraction.

AFM Sample Preparation

The metal single crystals were cleaned by repeated Ne^+ sputtering and annealing cycles. Bilayer NaCl islands were grown by subliming NaCl onto the clean metal substrate held at 277 K. Molecules were sublimed in situ from a silicon wafer onto the substrate held at ~ 10 K. CO for tip functionalization was dosed onto the substrate held at $T \approx 10$ K by admitting CO into the UHV system through a leak valve.

Atomic Force Microscopy

Noncontact AFM experiments (denoted as AFM) were carried out in a home-built, combined atomic force microscope/scanning tunneling microscope, operated in ultrahigh vacuum (UHV, base pressure $\sim 1 \times 10^{-10}$ mbar) and at low temperature ($T = 5$ K). AFM measurements were performed with a qPlus quartz force sensor (Giessibl, 1998) operated in the frequency-modulation mode (Albrecht et al., 1991). At $T = 5$ K, the force sensor had a resonance frequency of $f_0 = 28.8$ kHz and quality factor of $Q \approx 100,000$ and was operated at an oscillation amplitude of $A = 50$ pm. All AFM images were acquired in the constant height mode at a sample bias of $V = 0$ V with a CO-

functionalized tip. The typical acquisition time of such a noncontact AFM image is on the order of several minutes with a typical scanning speed of 1 nm s^{-1} . To functionalize the tip, we pick up a CO molecule from the NaCl islands by approaching the tip above a CO molecule, until a sudden change in the tunneling current signals the transfer of the CO from the surface to the tip. The CO molecule is maintained at the tip for imaging a molecule, and several molecules can be imaged with the same CO at the tip. However, the CO is often lost during the relatively large STM overview images. During overview images, tip changes frequently occur, observed as horizontal lines in Figs. 1a and 2a. These can be caused by mechanical contact with the surface or unintentionally picking up a molecule from the surface. Tip changes occurred more frequently for UM compared to EM.

Scanning Tunneling Microscopy

STM was performed in constant current mode, with the bias V applied to the sample with respect to the tip. Typically, a small tunneling current set point of $I = 1 \text{ pA}$ was chosen to reduce the occurrence of tip changes.

Fourier Transform Ion Cyclotron Resonance Mass Spectrometry

FTICR-MS experiments were carried out on a Solarix XR (Bruker Daltonics, Bremen, Germany) equipped with a 12 T superconducting magnet (Marshall & Chen, 2015; Nikolaev et al., 2011). LDI source (Nd:YAG $\times 3$ laser, 355 nm, 2000 Hz) was used to ionize both RM and EM using a previously reported work (Maillard et al., 2018). Spectra were acquired with a sum of 200 scans with a mass range of m/z 110–1200. Calibration and molecular assignments were carried out using DataAnalysis 5.1. Internal mass calibration was performed using confidently assigned signals, leading to a RMSE of 0.050 ppm. Molecular formulas were assigned considering the presence of maximum $\text{N}_3\text{O}_3\text{S}_3$ and a mass error of 0.2 ppm.

Acknowledgments—We thank Rolf Allenspach and Hassan Sabbah for helpful discussions. This work was supported by the ERC Consolidator Grant AMSEL (no. 682144), the ERC Synergy Grant MolDAM (no. 951519), the European FET-OPEN project SPRING (no. 863098), the H2020-MSCA-ITN ULTIMATE (no. 813036), the Spanish Agencia Estatal de Investigación (PCI2019-111933-2), Xunta de Galicia (Centro de Investigación de Galicia accreditation 2019–2022, ED431G 2019/03), the European Regional Development

Fund-ERDF and at COBRA Laboratory by the European Regional Development Fund (ERDF) N° HN0001343, the European Union's Horizon 2020 Research Infrastructures program (Grant Agreement 731077), and the Region Normandie, the Laboratoire d'Excellence (LabEx) SynOrg (ANR-11-LABX-0029). Access to a CNRS FTICR research infrastructure (FR3624) is gratefully acknowledged. A. S. B. acknowledges support from NASA's Planetary Science Division.

Data Availability Statement—The data that support the findings of this study are available from the corresponding author, L. G., upon reasonable request.

Editorial Handling—Dr. Daniel Glavin

REFERENCES

- Albrecht, F., Pavliček, N., Herranz-Lancho, C., Ruben, M., and Repp, J. 2015. Characterization of a Surface Reaction by Means of Atomic Force Microscopy. *Journal of the American Chemical Society* 137: 7424–8.
- Albrecht, T. R., Grütter, P., Horne, D., and Rugar, D. 1991. Frequency Modulation Detection Using High-Q Cantilevers for Enhanced Force Microscope Sensitivity. *Journal of Applied Physics* 69: 668–73.
- Alexander, C. M. O'D., Cody, G., De Gregorio, B., Nittler, L., and Stroud, R. 2017. The Nature, Origin and Modification of Insoluble Organic Matter in Chondrites, the Major Source of Earth's C and N. *Geochemistry* 77: 227–56.
- Alexander, C. M. O'D., Fogel, M., Yabuta, H., and Cody, G. 2007. The Origin and Evolution of Chondrites Recorded in the Elemental and Isotopic Compositions of Their Macromolecular Organic Matter. *Geochimica et Cosmochimica Acta* 71: 4380–403.
- Alexander, C. M. O'D., Russell, S., Arden, J., Ash, R., Grady, M., and Pillinger, C. 1998. The Origin of Chondritic Macromolecular Organic Matter: A Carbon and Nitrogen Isotope Study. *Meteoritics & Planetary Science* 33: 603–22.
- Alldrift, B., Hapala, P., Oinonen, N., Urtev, F., Krejci, O., Canova, F. F., Kannala, J., Schulz, F., Liljeroth, P., and Foster, A. S. 2020. Automated Structure Discovery in Atomic Force Microscopy. *Science Advances* 6: eaay6913.
- Aponte, J. C., Dworkin, J. P., and Elsila, J. E. 2014. Assessing the Origins of Aliphatic Amines in the Murchison Meteorite from Their Compound-Specific Carbon Isotopic Ratios and Enantiomeric Composition. *Geochimica et Cosmochimica Acta* 141: 331–45.
- Aponte, J. C., Elsila, J. E., Hein, J. E., Dworkin, J. P., Glavin, D. P., McLain, H. L., Parker, E. T., Cao, T., Berger, E. L., and Burton, A. S. 2020. Analysis of Amino Acids, Hydroxy Acids, and Amines in CR Chondrites. *Meteoritics & Planetary Science* 55: 2422–39.
- Aponte, J. C., Whitaker, D., Powner, M. W., Elsila, J. E., and Dworkin, J. P. 2019. Analyses of Aliphatic Aldehydes and Ketones in Carbonaceous Chondrites. *ACS Earth and Space Chemistry* 3: 463–72.

- Basile, B. P., Middleditch, B. S., and Oró, J. 1984. Polycyclic Aromatic Hydrocarbons in the Murchison Meteorite. *Organic Geochemistry* 5: 211–6.
- Beuhler, R., Flanigan, E., Greene, L., and Friedman, L. 1974. Proton Transfer Mass Spectrometry of Peptides. Rapid Heating Technique for Underivatized Peptides Containing Arginine. *Journal of the American Chemical Society* 96: 3990–9.
- Brearley, A. J. 2006. The Action of Water. *Meteorites and the Early Solar System II* 943: 587–624.
- Callahan, M. P., Smith, K. E., Cleaves, H. J., Ruzicka, J., Stern, J. C., Glavin, D. P., House, C. H., and Dworkin, J. P. 2011. Carbonaceous Meteorites Contain a Wide Range of Extraterrestrial Nucleobases. *Proceedings of the National Academy of Sciences* 108: 13995–8.
- Cho, Y., Kim, Z., and Kim, S. 2011. Planar Limit-Assisted Structural Interpretation of Saturates/Aromatics/Resins/Asphaltenes Fractionated Crude Oil Compounds Observed by Fourier Transform Ion Cyclotron Resonance Mass Spectrometry. *Analytical Chemistry* 83: 6068–73.
- Chyba, C. F., Thomas, P. J., Brookshaw, L., and Sagan, C. 1990. Cometary Delivery of Organic Molecules to the Early Earth. *Science* 249: 366–73.
- Cody, G. D., and Alexander, C. M. O'D. 2005. NMR Studies of Chemical Structural Variation of Insoluble Organic Matter from Different Carbonaceous Chondrite Groups. *Geochimica et Cosmochimica Acta* 69: 1085–97.
- Commodo, M., Kaiser, K., De Falco, G., Minutolo, P., Schulz, F., D'Anna, A., and Gross, L. 2019. On the Early Stages of Soot Formation: Molecular Structure Elucidation by High-Resolution Atomic Force Microscopy. *Combustion and Flame* 205: 154–64.
- Cooper, G., Kimmich, N., Belisle, W., Sarinana, J., Brabham, K., and Garrel, L. 2001. Carbonaceous Meteorites as a Source of Sugar-Related Organic Compounds for the Early Earth. *Nature* 414: 879–83.
- Danger, G., Ruf, A., Maillard, J., Hertzog, J., Vinogradoff, V., Schmitt-Kopplin, P., Afonso, C. et al. 2020. Unprecedented Molecular Diversity Revealed in Meteoritic Insoluble Organic Matter: The Paris Meteorite's Case. *The Planetary Science Journal* 1: 55.
- de Oteyza, D. G., Gorman, P., Chen, Y.-C., Wickenburg, S., Riss, A., Mowbray, D. J., Etkin, G. et al. 2013. Direct Imaging of Covalent Bond Structure in Single-Molecule Chemical Reactions. *Science* 340: 1434–7.
- Derenne, S., and Robert, F. 2010. Model of Molecular Structure of the Insoluble Organic Matter Isolated from Murchison Meteorite. *Meteoritics & Planetary Science* 45: 1461–75.
- Elsila, J. E., Aponte, J. C., Blackmond, D. G., Burton, A. S., Dworkin, J. P., and Glavin, D. P. 2016. Meteoritic Amino Acids: Diversity in Compositions Reflects Parent Body Histories. *ACS Central Science* 2: 370–9.
- Elsila, J. E., de Leon, N. P., Buseck, P. R., and Zare, R. N. 2005. Alkylation of Polycyclic Aromatic Hydrocarbons in Carbonaceous Chondrites. *Geochimica et Cosmochimica Acta* 69: 1349–57.
- Fatayer, S., Coppola, A. I., Schulz, F., Walker, B. D., Broek, T. A., Meyer, G., Druffel, E. R., McCarthy, M., and Gross, L. 2018. Direct Visualization of Individual Aromatic Compound Structures in Low Molecular Weight Marine Dissolved Organic Carbon. *Geophysical Research Letters* 45: 5590–8.
- Furukawa, Y., Chikaraishi, Y., Ohkouchi, N., Ogawa, N. O., Glavin, D. P., Dworkin, J. P., Abe, C., and Nakamura, T. 2019. Extraterrestrial Ribose and Other Sugars in Primitive Meteorites. *Proceedings of the National Academy of Sciences* 116: 24440–5.
- Giessibl, F. J. 1998. High-Speed Force Sensor for Force Microscopy and Profilometry Utilizing a Quartz Tuning Fork. *Applied Physics Letters* 73: 3956–8.
- Glavin, D. P., Alexander, C. M., Aponte, J. C., Dworkin, J. P., Elsila, J. E., and Yabuta, H. 2018. The Origin and Evolution of Organic Matter in Carbonaceous Chondrites and Links to Their Parent Bodies. In *Primitive Meteorites and Asteroids*, edited by N. Abreu, 205–71. Amsterdam: Elsevier.
- Gross, L., Mohn, F., Moll, N., Liljeroth, P., and Meyer, G. 2009. The Chemical Structure of a Molecule Resolved by Atomic Force Microscopy. *Science* 325: 1110–4.
- Gross, L., Mohn, F., Moll, N., Meyer, G., Ebel, R., Abdel-Mageed, W. M., and Jaspars, M. 2010. Organic Structure Determination Using Atomic Resolution Scanning Probe Microscopy. *Nature Chemistry* 2: 821–5.
- Gross, L., Mohn, F., Moll, N., Schuler, B., Criado, A., Guitián, E., Peña, D., Gourdon, A., and Meyer, G. 2012. Bond-Order Discrimination by Atomic Force Microscopy. *Science* 337: 1326–9.
- Gross, L., Schuler, B., Pavliček, N., Fatayer, S., Majzik, Z., Moll, N., Peña, D., and Meyer, G. 2018. Atomic Force Microscopy for Molecular Structure Elucidation. *Angewandte Chemie International Edition* 57: 3888–908.
- Hamann, C., Woltmann, R., Hong, I.-P., Hauptmann, N., Karan, S., and Berndt, R. 2011. Ultrahigh Vacuum Deposition of Organic Molecules by Electrospray Ionization. *Review of Scientific Instruments* 82: 033903.
- Hanssen, K. O., Schuler, B., Williams, A., Demissie, T. B., Hansen, E., Andersen, J. H., Svenson, J. et al. 2012. A Combined Atomic Force Microscopy and Computational Approach for Structural Elucidation of Breitfussin A and B, Highly Modified Halogenated Dipeptides from *Thuaria breitfussi*. *Angewandte Chemie International Edition* 51: 12238–41.
- Hapala, P., Kichin, G., Wagner, C., Tautz, F. S., Temirov, R., and Jelínek, P. 2014. The Mechanism of High-Resolution STM/AFM Imaging with Functionalized Tips. *Physical Review B* 90: 85421.
- Huang, Y., Wang, Y., Alexandre, M. R., Lee, T., Rose-Petrucci, C., Fuller, M., and Pizzarello, S. 2005. Molecular and Compound-Specific Isotopic Characterization of Monocarboxylic Acids in Carbonaceous Meteorites. *Geochimica et Cosmochimica Acta* 69: 1073–84.
- Maillard, J., Carrasco, N., Schmitz-Afonso, I., Gautier, T., and Afonso, C. 2018. Comparison of Soluble and Insoluble Organic Matter in Analogues of Titan's Aerosols. *Earth and Planetary Science Letters* 495: 185–91.
- Marshall, A. G., and Chen, T. 2015. 40 Years of Fourier Transform Ion Cyclotron Resonance Mass Spectrometry. *International Journal of Mass Spectrometry* 377: 410–20.
- Martínez, L., Santoro, G., Merino, P., Accolla, M., Lauwaet, K., Sobrado, J., Sabbah, H. et al. 2020. Prevalence of Non-Aromatic Carbonaceous Molecules in the Inner Regions of Circumstellar Envelopes. *Nature Astronomy* 4: 97–105.
- Martin-Jimenez, D., Ahles, S., Mollenhauer, D., Wegner, H. A., Schirmeisen, A., and Ebeling, D. 2019. Bond-Level Imaging of the 3D Conformation of Adsorbed Organic

- Molecules Using Atomic Force Microscopy with Simultaneous Tunneling Feedback. *Physical Review Letters* 122: 196101.
- Mohn, F., Gross, L., and Meyer, G. 2011. Measuring the Short-Range Force Field Above a Single Molecule with Atomic Resolution. *Applied Physics Letters* 99: 053106.
- Moll, N., Gross, L., Mohn, F., Curioni, A., and Meyer, G. 2010. The Mechanisms Underlying the Enhanced Resolution of Atomic Force Microscopy with Functionalized Tips. *New Journal of Physics* 12: 125020.
- Moll, N., Gross, L., Mohn, F., Curioni, A., and Meyer, G. 2012. A Simple Model of Molecular Imaging with Noncontact Atomic Force Microscopy. *New Journal of Physics* 14: 83023.
- Moreno, C., Stetsovych, O., Shimizu, T. K., and Custance, O. 2015. Imaging Three-Dimensional Surface Objects with Submolecular Resolution by Atomic Force Microscopy. *Nano Letters* 15: 2257–62.
- Nikolaev, E. N., Boldin, I. A., Jertz, R., and Baykut, G. 2011. Initial Experimental Characterization of a New Ultra-High Resolution FTICR Cell with Dynamic Harmonization. *Journal of the American Society of Mass Spectrometry* 22: 1125–33.
- Oró, J. 1961. Comets and the Formation of Biochemical Compounds on the Primitive Earth. *Nature* 190: 389–90.
- Pavliček, N., Mistry, A., Majzik, Z., Moll, N., Meyer, G., Fox, D. J., and Gross, L. 2017. Synthesis and Characterization of Triangulene. *Nature Nanotechnology* 12: 308–11.
- Pawlak, R., Vilhena, J., Hinaut, A., Meier, T., Glatzel, T., Baratoff, A., Gnecco, E., Pérez, R., and Meyer, E. 2019. Conformations and Cryo-Force Spectroscopy of Spray-Deposited Single-Strand DNA on Gold. *Nature Communications* 10: 1–7.
- Pearson, V., Sephton, M., Franchi, I., Gibson, J., and Gilmour, I. 2006. Carbon and Nitrogen in Carbonaceous Chondrites: Elemental Abundances and Stable Isotopic Compositions. *Meteoritics & Planetary Science* 41: 1899–918.
- Pering, K. L., and Ponnampuruma, C. 1971. Aromatic Hydrocarbons in the Murchison Meteorite. *Science* 173: 237–9.
- Pizzarello, S. 2007. The Chemistry That Preceded Life's Origin: A Study Guide from Meteorites. *Chemistry & Biodiversity* 4: 680–93.
- Pizzarello, S., Cooper, G., and Flynn, G. 2006. The Nature and Distribution of the Organic Material in Carbonaceous Chondrites and Interplanetary Dust Particles. In *Meteorites and the Early Solar System II*, edited by D. S. Lauretta and H. Y. McSween, Vol. 1, 625–51. Tucson, Arizona: University of Arizona Press.
- Pizzarello, S., and Huang, Y. 2002. Molecular and Isotopic Analyses of Tagish Lake Alkyl Dicarboxylic Acids. *Meteoritics & Planetary Science* 37: 687–96.
- Pizzarello, S., Huang, Y., Becker, L., Poreda, R. J., Nieman, R. A., Cooper, G., and Williams, M. 2001. The Organic Content of the Tagish Lake Meteorite. *Science* 293: 2236–9.
- Rapenne, G., Grill, L., Zambelli, T., Stojkovic, S., Ample, F., Moresco, F., and Joachim, C. 2006. Launching and Landing Single Molecular Wheelbarrows on a Cu (1 0 0) Surface. *Chemical Physics Letters* 431: 219–22.
- Rauschenbach, S., Vogelgesang, R., Malinowski, N., Gerlach, J. W., Benyoucef, M., Costantini, G., Deng, Z., Thontasen, N., and Kern, K. 2009. Electrospray Ion Beam Deposition: Soft-Landing and Fragmentation of Functional Molecules at Solid Surfaces. *ACS Nano* 3: 2901–10.
- Remusat, L., Derenne, S., Robert, F., and Knicker, H. 2005. New Pyrolytic and Spectroscopic Data on Orgueil and Murchison Insoluble Organic Matter: A Different Origin Than Soluble? *Geochimica et Cosmochimica Acta* 69: 3919–32.
- Ruf, A., Poinot, P., Geffroy, C., d'Hendecourt, L. L. S., and Danger, G. 2019. Data-Driven UPLC-Orbitrap MS Analysis in Astrochemistry. *Life* 9: 35.
- Sandford, S. A., Nuevo, M., Bera, P. P., and Lee, T. J. 2020. Prebiotic Astrochemistry and the Formation of Molecules of Astrobiological Interest in Interstellar Clouds and Protostellar Disks. *Chemical Reviews* 120: 4616–59.
- Santoro, G., Martnez, L., Lauwaet, K., Accolla, M., Tajuelo-Castilla, G., Merino, P., Sobrado, J. M. et al. 2020. The Chemistry of Cosmic Dust Analogs from C, C₂, and C₂H₂ in C-Rich Circumstellar Envelopes. *The Astrophysical Journal* 895: 97.
- Schmitt-Kopplin, P., Gabelica, Z., Gougeon, R. d., Fekete, A., Kanawati, B., Harir, M., Gebefuegi, I., Eckel, G., and Hertkorn, N. 2010. High Molecular Diversity of Extraterrestrial Organic Matter in Murchison Meteorite Revealed 40 Years After Its Fall. *Proceedings of the National Academy of Sciences* 107: 2763–8.
- Schmitt-Kopplin, P., Hemmler, D., Moritz, F., Gougeon, R. D., Lucio, M., Meringer, M., Müller, C., Harir, M., and Hertkorn, N. 2019. Systems Chemical Analytics: Introduction to the Challenges of Chemical Complexity Analysis. *Faraday Discussions* 218: 9–28.
- Schuler, B., Fatayer, S., Meyer, G., Rogel, E., Moir, M., Zhang, Y., Harper, M. R. et al. 2017. Heavy Oil Based Mixtures of Different Origins and Treatments Studied by AFM. *Energy & Fuels* 31: 6856–61.
- Schuler, B., Fatayer, S., Mohn, F., Moll, N., Pavliček, N., Meyer, G., Peña, D., and Gross, L. 2016. Reversible Bergman Cyclization by Atomic Manipulation. *Nature Chemistry* 8: 220–4.
- Schuler, B., Liu, W., Tkatchenko, A., Moll, N., Meyer, G., Mistry, A., Fox, D., and Gross, L. 2013. Adsorption Geometry Determination of Single Molecules by Atomic Force Microscopy. *Physical Review Letters* 111: 106103.
- Schuler, B., Meyer, G., Peña, D., Mullins, O. C., and Gross, L. 2015. Unraveling the Molecular Structures of Asphaltenes by Atomic Force Microscopy. *Journal of the American Chemical Society* 137: 9870–6.
- Schuler, B., Mohn, F., Gross, L., Meyer, G., and Jaspars, M. 2015. Prospects and Challenges in Molecular Structure Identification by Atomic Force Microscopy. In *Modern NMR Approaches to the Structure Elucidation of Natural Products: Volume 1: Instrumentation and Software*, edited by A. J. Williams, G. E. Martin and D. Rovnyak, 306–20. Cambridge, UK: Royal Chemical Society.
- Schuler, B., Zhang, Y., Collazos, S., Fatayer, S., Meyer, G., Pérez, D., Guitián, E. et al. 2017. Characterizing Aliphatic Moieties in Hydrocarbons with Atomic Force Microscopy. *Chemical Science* 8: 2315–20.
- Schuler, B., Zhang, Y., Liu, F., Pomerantz, A. E., Andrews, A. B., Gross, L., Pauchard, V., Banerjee, S., and Mullins, O. C. 2020. Overview of Asphaltene Nanostructures and Thermodynamic Applications. *Energy & Fuels* 34: 15082–105.

- Schulz, F., Maillard, J., Kaiser, K., Schmitz-Afonso, I., Gautier, T., Afonso, C., Carrasco, N., and Gross, L. 2021. Imaging Titan's Organic Haze at Atomic Scale. *The Astrophysical Journal Letters* 908: L13.
- Schulz, F., Ritala, J., Krejci, O., Seitsonen, A. P., Foster, A. S., and Liljeroth, P. 2018. Elemental Identification by Combining Atomic Force Microscopy and Kelvin Probe Force Microscopy. *ACS Nano* 12: 5274–83.
- Sephton, M. A. 2002. Organic Compounds in Carbonaceous Meteorites. *Natural Product Reports* 19: 292–311.
- Sephton, M., Pillinger, C., and Gilmour, I. 1998. $\delta^{13}\text{C}$ of Free and Macromolecular Aromatic Structures in the Murchison Meteorite. *Geochimica et Cosmochimica Acta* 62: 1821–8.
- Sephton, M., Pillinger, C., and Gilmour, I. 2001. Supercritical Fluid Extraction of the Non-Polar Organic Compounds in Meteorites. *Planetary and Space Science* 49: 101–6.
- Simkus, D. N., Aponte, J. C., Hilt, R. W., Elsilá, J. E., and Herd, C. D. 2019. Compound-Specific Carbon Isotope Compositions of Aldehydes and Ketones in the Murchison Meteorite. *Meteoritics & Planetary Science* 54: 142–56.
- Stanford, L. A., Kim, S., Rodgers, R. P., and Marshall, A. G. 2006. Characterization of Compositional Changes in Vacuum Gas Oil Distillation Cuts by Electrospray Ionization Fourier Transform-Ion Cyclotron Resonance (FT-ICR) Mass Spectrometry. *Energy & Fuels* 20: 1664–73.
- Van Der Heijden, N. J., Hapala, P., Rombouts, J. A., van der Lit, J., Smith, D., Mutombo, P., Svec, M., Jelinek, P., and Swart, I. 2016. Characteristic Contrast in Δf_{min} Maps of Organic Molecules Using Atomic Force Microscopy. *ACS Nano* 10: 8517–25.
- Zahl, P., and Zhang, Y. 2019. Guide for Atomic Force Microscopy Image Analysis to Discriminate Heteroatoms in Aromatic Molecules. *Energy & Fuels* 33: 4775–80.
- Zhang, Y., Schuler, B., Fatayer, S., Gross, L., Harper, M. R., and Kushnerick, J. D. 2018. Understanding the Effects of Sample Preparation on the Chemical Structures of Petroleum Imaged with Non-Contact Atomic Force Microscopy. *Industrial and Engineering Chemistry Research* 57: 15935–41.

SUPPORTING INFORMATION

Additional supporting information may be found in the online version of this article.

Fig. S1. Additional AFM images at different tip-sample distances for EM1–EM5 (a–e) and EM8 (f) from large (left) to small tip-sample distances (right) together with their corresponding Laplace-filtered images. The tip-height offset Δz with respect to the STM setpoint is given for each pair of images, with positive Δz indicating an increase in tip-sample distance. The STM setpoints that were used (sample voltage V and tunneling current I) were 0.4 V, 1 pA (EM1), 0.5 V, 1 pA (EM2 and EM4), 0.2 V, 1 pA (EM3 and EM8), and 0.2 V, 0.8 pA (EM5). The scale bars correspond to 0.5 nm and apply to all images.

Fig. S2. Comparison of experimental and simulated AFM images of EM5. a) Experimental AFM images at different tip-sample distances together with the corresponding Laplace-filtered data and proposed chemical structure overlaid on the first AFM image. b) Simulated AFM images of the proposed structure created with the probe particle model from large (left) to small (right) tip-sample distances in steps of 0.1 Å. The scale bar in (a) corresponds to 0.5 nm and applies to all images.

Fig. S3. Comparison between RM and EM at two different nominal masses, 266 and 267. Molecular formulas of several species are given for each sample.

Fig. S4. DBE versus carbon number plots of the O1 and S1 heteroatomic family for each sample: (a) O1 of the EM, (b) O1 of the RM, (c) S1 of the EM, and (d) S1 of the RM.